Chin. Phys. Lett. **39**, 067402 (2022)

First-Principles Study of Hole-Doped Superconductors $R\mathrm{NiO_2}$ (R = Nd, La, and Pr)

Juan-Juan Hao(蒿娟娟)[1†], Pei-Han Sun(孙培函)[2†], Ming Zhang(张铭)[1], Xian-Xin Wu(吴贤新)[3,4*], Kai Liu(刘凯)[2*], and Fan Yang(杨帆)[1*]

[1]*School of Physics, Beijing Institute of Technology, Beijing 100081, China*
[2]*Department of Physics and Beijing Key Laboratory of Opto-electronic Functional Materials & Micro-nano Devices, Renmin University of China, Beijing 100872, China*
[3]*CAS Key Laboratory of Theoretical Physics, Institute of Theoretical Physics, Chinese Academy of Sciences, Beijing 100190, China*
[4]*Max-Planck-Institut für Festkörperforschung, Heisenbergstrasse 1, D-70569 Stuttgart, Germany*

(Received 18 March 2022; accepted 2 May 2022; published online 29 May 2022)

Recent experiments have found that in contrast to the nonsuperconducting bulk $R\mathrm{NiO_2}$ (R = Nd, La, and Pr), the strontium-doped $R_{1-x}\mathrm{Sr}_x\mathrm{NiO_2}$ thin films show superconductivity with the critical temperature T_c of 9–15 K at $x = 0.2$, whose origin of superconductivity deserves further investigation. Based on first-principles calculations, we study the electronic structure, lattice dynamics, and electron–phonon coupling (EPC) of the undoped and doped $R\mathrm{NiO_2}$ (R = Nd, La, and Pr) at the experimental doping level. Our results show that the EPC-derived T_c's are all about 0 K in the undoped and doped $R\mathrm{NiO_2}$. The electron–phonon coupling strength is too small to account for the observed superconductivity. We hence propose that the electron–phonon interaction can not be the exclusive origin of the superconductivity in $R\mathrm{NiO_2}$ (R = Nd, La, and Pr).

DOI: 10.1088/0256-307X/39/6/067402

Superconducting materials with high transition temperature (T_c) have been explored for many years. Traditionally, the pairing mechanism of superconductivity is described by the Bardeen–Cooper–Schrieffer (BCS) theory,[1] in which the phonons mediate the effective attraction between a Cooper pair through the electron–phonon coupling (EPC). Superconductors that can be well described by the BCS theory are usually referred to as conventional superconductors, such as Hg,[2] $\mathrm{MgB_2}$,[3] and $\mathrm{LaH_{10}}$,[4] and the remaining ones are called unconventional superconductors.[5] Their differences lie in the formation mechanism of Cooper pairs[6] and the symmetry of the superconducting gap function. For example, in copper oxide superconductors, the superconducting gap is anisotropic and d-wave,[7] and the formation of Cooper pairs is not caused by electron–phonon interactions, but may be related to magnetic fluctuations.[8]

Recently, enormous attention has been paid to the research of undoped and hole-doped[9–39] infinite-layer nickelates $R\mathrm{NiO_2}$ (R = Nd, La, and Pr) from soft-chemistry topotactic reduction. Experiments show that, for $R\mathrm{NiO_2}$ (R = Nd, La, and Pr) materials, the hole doped $R\mathrm{NiO_2}$ thin films exhibit superconductivity,[18–20] while bulk $R\mathrm{NiO_2}$ does not.[39] For example, the infinite layer of strontium-doped $\mathrm{NdNiO_2}$ film ($\mathrm{Nd_{0.8}Sr_{0.2}NiO_2}$) is found to be superconducting and its critical temperature T_c reaches up to 15 K.[18] For $\mathrm{La_{1-x}Sr_xNiO_2}$ ($x = 0.14$–0.20), a superconducting transition follows, and the maximum T_c (9 K) occurs at $x = 0.20$.[19] In the $\mathrm{PrNiO_2}$ film synthesized on an $\mathrm{SrTiO_3}$ substrate, it was observed that the phase transition temperature of $\mathrm{Pr_{0.8}Sr_{0.2}NiO_2}$ superconductor is 7–12 K.[20] Previous calculations[11] suggest that the EPC strength in undoped $\mathrm{NdNiO_2}$ is not strong enough to regulate superconductivity around $T_\mathrm{c} \sim 10$ K and the EPC is excluded as the only source of superconductivity. However, experimentally undoped $\mathrm{NdNiO_2}$ itself is not superconducting. Hence, in order to explain the origin of superconductivity in doped $R\mathrm{NiO_2}$ (R = Nd, La, and Pr), it is actually more reasonable to study it with the hole doping.

According to the above experiments, the optimal hole doping in $R\mathrm{NiO_2}$ is 0.2 with the maximum transition temperature T_c about 15 K.[18–20] Therefore, we choose the 0.2 hole-doping case to verify whether the superconductivities of $\mathrm{NdNiO_2}$ and its sister compounds $\mathrm{LaNiO_2}$ and $\mathrm{PrNiO_2}$ originate from EPC. Based on the first-principles calculations and the EPC theory, we have made a comparative study on the electronic structure, phonon properties, EPC strength, and superconducting transition temperature of $R\mathrm{NiO_2}$ (R = Nb, La, and Pr) under the undoped

†Juan-Juan Hao and Pei-Han Sun contributed equally to this work.
*Corresponding author. Email: xianxinwu@gmail.com; kliu@ruc.edu.cn; yangfan_blg@bit.edu.cn
© 2022 Chinese Physical Society and IOP Publishing Ltd

and hole-doped conditions.

The electronic structure, phonon spectrum, and EPC of undoped and doped RNiO$_2$ (R = Nd, La, and Pr) were calculated by using Quantum ESPRESSO (QE) package[40] based on density functional theory[41,42] and density functional perturbation theory.[43] The generalized gradient approximation of Perdew–Burke–Ernzerhof type[44] was adopted for the exchange-correlation functional. The interactions between electrons and nuclei were described by the projected augmented wave method as implemented in PSlibrary.[45] The kinetic energy cutoff of the plane-wave function is 75 Ry and that of the charge density is 600 Ry. Both lattice constants and internal atomic positions were fully optimized. The hole doping effect was simulated by directly removing electrons from the system together with a compensating uniform charge background to maintain the charge neutrality. A $12 \times 12 \times 12$ k-grid was used for the self-consistent calculations. In the calculations of the dynamical matrix and the EPC, the Brillouin zone was sampled with a $6\times6\times6$ q-grid and a dense $48\times48\times48$ k-point mesh.

Based on the BCS theory,[1] the Eliashberg spectral function $\alpha^2F(\omega)$ is defined as[46]

$$\alpha^2F(\omega) = \frac{1}{2\pi N(\varepsilon_{\rm F})}\sum_{q\nu}\delta(\omega-\omega_{q\nu})\frac{\gamma_{q\nu}}{\hbar\omega_{q\nu}}, \quad (1)$$

where $N(\varepsilon_{\rm F})$ is the density of states (DOS) at Fermi level $\varepsilon_{\rm F}$, $\omega_{q\nu}$ is the frequency of the νth phonon mode at wave vector q, and $\gamma_{q\nu}$ is the phonon linewidth. The total EPC constant λ can be obtained by[46]

$$\lambda = \sum_{q\nu}\lambda_{q\nu} = 2\int\frac{\alpha^2F(\omega)}{\omega}d\omega. \quad (2)$$

The superconducting transition temperature $T_{\rm c}$ can be determined by substituting the EPC constant λ into the McMillan–Allen–Dynes formula,[47]

$$T_{\rm c} = \frac{\omega_{\log}}{1.2}\exp\Big[\frac{-1.04(1+\lambda)}{\lambda(1-0.62\mu^*)-\mu^*}\Big], \quad (3)$$

where the logarithmic average of Eliashberg spectral function $\omega_{\log}$ is defined as

$$\omega_{\log} = \exp\Big[\frac{2}{\lambda}\int\frac{d\omega}{\omega}\alpha^2F(\omega)\ln(\omega)\Big], \quad (4)$$

and μ^* is the effective screened Coulomb repulsion constant with the empirical values between 0.08 and 0.15.[48,49] In our calculation, μ^* was set to 0.1.

The tetragonal crystal structure of infinite-layer nickelates RNiO$_2$ (R = Nd, La, and Pr) with the space group $P4/mmm$ (No. 123) is shown in Fig. 1(a). Taking the NdNiO$_2$ as an example, the optimized lattice constants of undoped case are a = 3.893 Å and c = 3.267 Å, in good accordance with the reported experimental data.[50] With a doping concentration of 0.2 holes per formula unit (f.u.), the lattice constants decrease slightly to a = 3.809 Å and c = 3.186 Å, which is also consistent with the measured data.[11] Figure 1(b) displays the Brillouin region (BZ) of the primitive cell along with the high-symmetry k points.

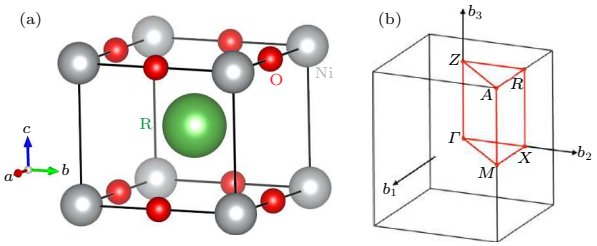

Fig. 1. (a) Crystal structure of RNiO$_2$ (R = Nd, La, and Pr) and (b) Brillouin zone of the primitive cell along with the high-symmetry paths labeled by red lines.[11]

Table 1. The lattice parameters, electronic density of states, EPC parameters, and superconducting $T_{\rm c}$ of RNiO$_2$ (R = Nd, La, and Pr) without doping and with a doping concentration of 0.2 holes/f.u. Here x is the doping concentration, a and c are the respective in-plane and out-of-plane lattice constants (in units of Å), $N(0)$ (in units of states/eV) represents the electronic density of states at the Fermi level, $\omega_{\log}$ (in units of cm^{-1}) represents the logarithmic average of the Eliashberg spectral function, σ is the width of the Gaussian smearing and λ denotes the EPC constant. Superconducting transition temperatures $T_{\rm c}$ (in units of K) were calculated with the McMillan–Allen–Dynes formula.[47]

	x	a	c	$N(0)$	$\omega_{\log}$	σ	λ	$T_{\rm c}$
NdNiO$_2$	0.0	3.894	3.267	1.43	230	0.015	0.172	0.0
NdNiO$_2$	0.2	3.809	3.186	1.26	283	0.010	0.128	0.0
LaNiO$_2$	0.0	3.935	3.387	1.38	235	0.015	0.167	0.0
LaNiO$_2$	0.2	3.850	3.308	1.18	285	0.020	0.127	0.0
PrNiO$_2$	0.0	3.907	3.309	1.45	235	0.015	0.168	0.0
PrNiO$_2$	0.2	3.822	3.230	1.27	288	0.020	0.127	0.0

Figure 2 shows the electronic band structure, density of states (DOS), and Fermi surfaces of NdNiO$_2$ without doping and with a doping concentration of 0.2 holes/f.u., respectively. As can be seen from Fig. 2(a), there are two bands passing through the Fermi level, indicating its metallic property. To analyze the orbital composition of these two bands, we projected them onto the 5d orbitals of Nd and the 3d orbitals of Ni, represented by green and blue dots, respectively. The first band is mainly contributed by Nd 5d orbitals, while the second one is mainly contributed by Ni 3d orbitals. By comparing the bands before and after doping, we find that the 0.2 holes/f.u. doping does not change the overall shape of the band structure, but causes an upward shift of the band structure relative to the Fermi level $E_{\rm F}$. According to the DOS [Fig. 2(b)], the electronic states around the $E_{\rm F}$ are mainly contributed by Ni 3d orbitals, while the contributions of Nd 5d orbitals and O 2p orbitals are minor. The inset in Fig. 2(b) shows the PDOS of Ni

$3d$ orbitals in undoped $NdNiO_2$. We can see that it is composed mainly of $3d_{x^2-y^2}$ at E_F. In addition, we find that the 0.2 hole doping can effectively reduce the total DOS at E_F. The same results are also observed for $LaNiO_2$ and $PrNiO_2$ (Table 1). From Fig. 2(c), the Fermi surface of undoped $NdNiO_2$ consists of two spherical electron pockets at the BZ center and the BZ corner, as well as a large barrel-like hole pocket in the BZ interior. Among them, the small electron pocket at the BZ center is mainly composed of Nd $5d$ orbitals, while the large hole pocket is mainly contributed by Ni $3d_{x^2-y^2}$ orbitals. Comparing Figs. 2(c) and 2(d), we find that these two electron-type Fermi surfaces shrink when the holes are doped in the material. This is consistent with the observed changes in electronic band structure with hole doping [Fig. 2(a)].

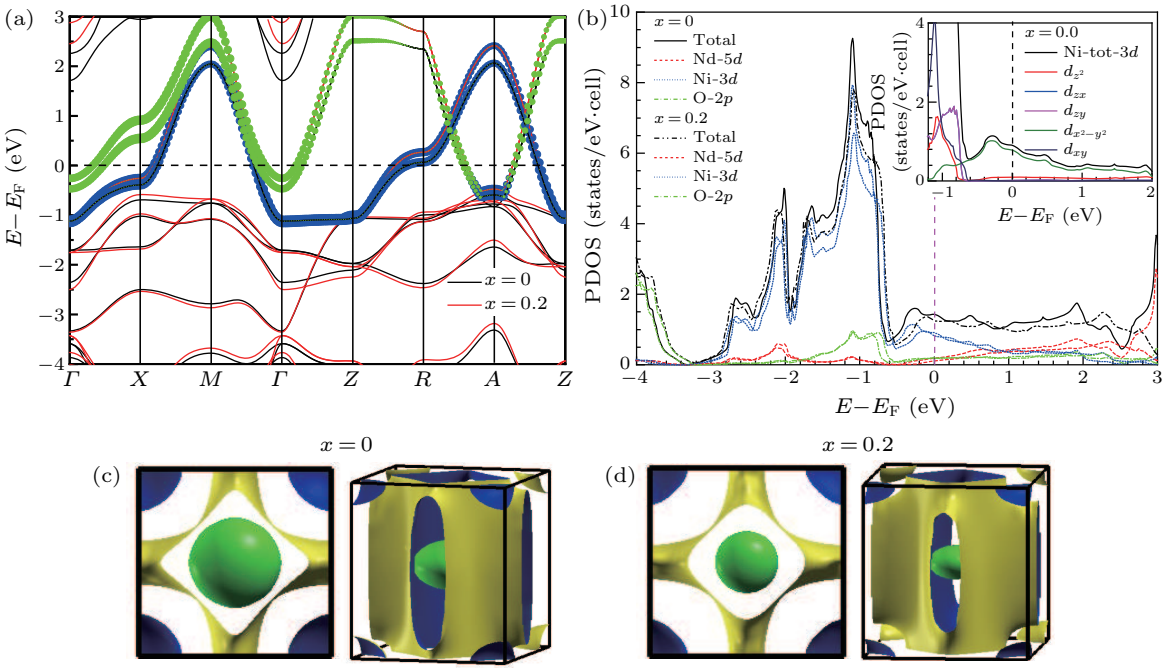

Fig. 2. (a) Electronic band structure of $NdNiO_2$ without doping (black lines) and with a doping concentration of 0.2 holes per formula unit (red lines). The two bands across the Fermi level E_F are projected onto the Nd $5d$ and Ni $3d$ orbitals and denoted with green and blue dots, respectively. The size of the dots is proportional to the weights of the corresponding orbitals. (b) Total and partial density of states (PDOS) without doping (solid lines) and after doping (dashed lines). Inset shows the PDOS of Ni $3d$ orbitals in undoped $NdNiO_2$. [(c), (d)] The top and three-dimensional side views of the Fermi surfaces without and with doping, respectively.

We next explore the phonon properties and the EPC of undoped and doped $RNiO_2$ (R = Nd, La, and Pr). We also take $NdNiO_2$ as an example to illustrate our results. Figures 3(a) and 3(d) show the phonon spectra before and after hole doping, respectively. We can see that there is no imaginary phonon mode in the whole BZ, indicating that they are both dynamically stable. In addition, we find that the phonon spectrum is hardened significantly after the hole doping, for which the maximum phonon frequency increases from 566 cm^{-1} to 641 cm^{-1}. This is also reflected in the change in ω_{log} (Table 1), which goes from 230 cm^{-1} to 283 cm^{-1} with the hole doping. The phonon density of states of undoped and doped $NdNiO_2$ are displayed in Figs. 3(b) and 3(e), respectively. We learn that the low-frequency branches are mainly contributed by the vibrations of Nd and Ni atoms, while the high-frequency branches are dominated by the O atomic vibrations.

The calculated Eliashberg spectral function $\alpha^2F(\omega)$ and integrated EPC constant λ of undoped and doped $NdNiO_2$ are shown in Figs. 3(c) and 3(f), respectively. It can be seen that the integrated $\lambda(\omega)$ (the red curve) decreases significantly after doping. Meanwhile, the peak at around 100 cm^{-1} in $\alpha^2F(\omega)$ also reduces remarkably. The calculated total EPC constant λ of undoped $NdNiO_2$ is only 0.172, which is further reduced to 0.128 with the hole doping of $x = 0.2$. Such reduction of λ can be attributed to the hardening of phonon spectra and the decrease of $\alpha^2F(\omega)$ [Fig. 3 and Eq. (2)]. Based on the McMillan–Allen–Dynes formula [Eq. (3)], we obtain the superconducting T_c's of both undoped and doped $NdNiO_2$ as nearly 0 K, see Table 1. Meanwhile, the calculated T_c's of $LaNiO_2$ and $PrNiO_2$ also approach 0 K in the undoped and doped cases. In order to display the influence of hole doping on T_c, the values are re-represented by scientific notation, with their actual values and orders of magnitude. Take $NdNiO_2$ as an example, the T_c is 6.452×10^{-7} K before doping and

1.373×10^{-23} K after doping. Obviously, the latter is much less than the former, which indicates that the EPC is not suitable for this system. The same results were also observed in $LaNiO_2$ and $PrNiO_2$. The fact that the hole doping suppresses EPC contradicts with the fact that hole doping induces superconductivity in experiments.[18–20] These suggests that the superconducting origin in hole-doped RNiO$_2$ is unlikely to be EPC-dominated.

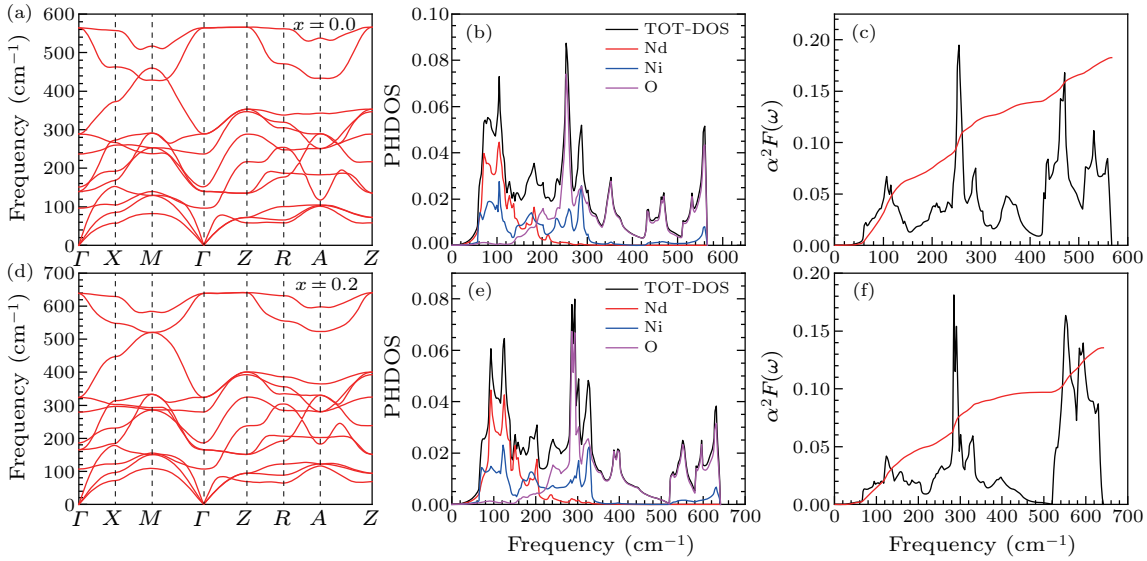

Fig. 3. Phonon and EPC properties of $NdNiO_2$ without doping and with a doping concentration of 0.2 holes per formula unit. [(a), (d)] Undoped and doped phonon band structures. [(b), (e)] Undoped and doped phonon DOSs with atomic projection. [(c), (f)] Eliashberg function $\alpha^2F(\omega)$ for the undoped and doped cases, respectively. The solid red lines represent the cumulative values of $\lambda(\omega)$.

Note that in experiments, superconductivity is only found in thin films[18–20] instead of bulk materials,[39] which implies the special role of the interface in promoting superconductivity. Here we only focus on the bulk materials as the first-principle calculations for the thin films with substrates are difficult to perform. We leave such a topic for future study.

In summary, we have systematically studied the electronic, phonon, and superconducting properties of undoped and doped RNiO$_2$ (R = Nd, La, and Pr) using first-principles calculations. The effect of hole doping induces an overall upward shift of the electronic bands, the contraction of the electron-type Fermi pockets, and the significant reduction of DOS at E_F. At the same time, the hole doping can harden the phonon spectrum and reduce the EPC constant effectively. All calculated superconducting T_c's remain 0 K for RNiO$_2$ with and without hole doping, which means that this kind of materials does not comply with the EPC mechanism of the BCS theory. Our theoretical calculations thus fully prove that RNiO$_2$ (R = Nd, La, and Pr) superconductors after hole doping belong to the unconventional superconductors.

Acknowledgments. This work was supported by the National Natural Science Foundation of China (Grant Nos. 12074031, 11674025, and 12174443), the National Key R&D Program of China (Grant No. 2017YFA0302903), and the Beijing Natural Science Foundation (Grant No. Z200005).

References

[1] Bardeen J, Cooper L N and Schrieffer J R 1957 *Phys. Rev.* **108** 1175
[2] Kamerlingh Onnes H 1911 *Commun. Phys. Lab. Univ. Leiden* **122** 122
[3] Drozdov A P, Kong P P, Minkov V S, Besedin S P, Kuzovnikov M A, Mozaffari S, Balicas L, Balakirev F F, Graf D E, Prakapenka V B, Greenberg E, Knyazev D A, Tkacz M and Eremets M I 2019 *Nature* **569** 528
[4] Nagamatsu J, Nakagawa N, Muranaka T, Zenitani Y and Akimitsu J 2001 *Nature* **410** 63
[5] Sigrist M and Ueda K 1991 *Rev. Mod. Phys.* **63** 239
[6] Cooper L N 1956 *Phys. Rev.* **104** 1189
[7] Harlingen V D J 1995 *Rev. Mod. Phys.* **67** 515
[8] Anderson P W 1987 *Science* **235** 1196
[9] Wu X X, Sante D D, Schwemmer T, Hanke W, Hwang H Y, Raghu S and Thomale R 2020 *Phys. Rev. B* **101** 060504
[10] Bandyopadhyay S, Adhikary P, Das T, Dasgupta I and Saha-Dasgupta T 2020 *Phys. Rev. B* **102** 220502
[11] Nomura Y, Hirayama M, Tadano T, Yoshimoto Y, Nakamura K and Arita R 2019 *Phys. Rev. B* **100** 205138
[12] Botana A S and Norman M R 2020 *Phys. Rev. X* **10** 011024
[13] Zhang M, Zhang Y, Guo H and Yang F 2021 *Chin. Phys. B* **30** 108204
[14] Zhang X M and Li B 2022 *J. Solid State Chem.* **306** 122806
[15] Jiang P, Si L, Liao Z and Zhong Z 2019 *Phys. Rev. B* **100** 201106
[16] Lin H, Gawryluk D J, Klein Y M, Huangfu S, Pomjakushina E, von Rohr F and Schilling A 2022 *New J. Phys.* **24** 013022
[17] Gu Y, Zhu S, Wang X H J and Chen H 2020 *Commun. Phys.* **3** 84
[18] Li D, Lee K, Wang B Y, Osada M, Crossley S, Lee H R, Cui Y, Hikita Y and Hwang H Y 2019 *Nature* **572** 624
[19] Osada M, Wang B Y, Goodge B H, Harvey S P, Lee K, Li D and Hwang H Y 2021 *Adv. Mater.* **33** 2104083

[20] Osada M, Wang B Y, Goodge B H, Lee K, Yoon H, Sakuma K, Li D, Miura M, Kourkoutis L F and Hwang H Y 2020 *Nano Lett.* **20** 5735
[21] Ryee S, Yoon H, Kim T J, Jeong M Y and Han M J 2020 *Phys. Rev. B* **101** 064513
[22] Li D, Wang B Y, Lee K, Harvey S P, Osada M, Goodge B H and Hwang H Y 2020 *Phys. Rev. Lett.* **125** 027001
[23] Gu Q, Li Y, Wan S, Li H, Guo W, Yang H and Wen H H 2020 *Nat. Commun.* **11** 6027
[24] Li Q, He C, Si J, Zhu X, Zhang Y and Wen H H 2020 *Commun. Mater.* **1** 16
[25] Osada M, Wang B Y, Lee K, Li D and Hwang H Y 2020 *Phys. Rev. Mater.* **4** 121801
[26] Zeng S, Tang C S, Yin X, Li C, Li M, Huang Z and Ariando A 2020 *Phys. Rev. Lett.* **125** 147003
[27] Zhang H, Jin L, Wang S, Xi B, Shi X, Ye F and Mei J W 2020 *Phys. Rev. Res.* **2** 013214
[28] Wang Y, Kang C J, Miao H and Kotliar G 2020 *Phys. Rev. B* **102** 161118
[29] Kang C J and Kotliar G 2021 *Phys. Rev. Lett.* **126** 127401
[30] Lechermann F 2020 *Phys. Rev. X* **10** 041002
[31] Gu Q and Wen H 2021 *Innovation* **3** 100202
[32] Talantsev E F 2020 *Results Phys.* **17** 103118
[33] Ying X *et al.* 2021 *Chin. Phys. Lett.* **38** 047401
[34] Lechermann F 2021 *Phys. Rev. Mater.* **5** 044803
[35] Zhou X R, Feng Z X, Qin P X, Yan H, Wang X N, Nie P and Liu Z Q 2021 *Rare Met.* **40** 2847
[36] Leonov I 2021 *J. Alloys Compd.* **883** 160888
[37] Botana A S, Bernardini F and Cano A 2021 *J. Exp. Theor. Phys.* **132** 618
[38] LaBollita H and Botana A S 2022 *Phys. Rev. B* **105** 085118
[39] Wang B X, Zheng H, Krivyakina E, Chmaissem O, Lopes P P, Lynn J W and Phelan D 2020 *Phys. Rev. Mater.* **4** 084409
[40] Giannozzi P, Andreussi O, Brumme T, Bunau O, Nardelli M B, Calandra M, Car R, Cavazzoni C, Ceresoli D, Cococcioni M and Baroni S 2017 *J. Phys. Condens. Matter* **29** 465901
[41] Hohenberg P and Kohn W 1964 *Phys. Rev.* **136** B864
[42] Kohn W and Sham L J 1965 *Phys. Rev.* **140** A1133
[43] Baroni S, de Gironcoli S, Dal C A and Giannozzi P 2001 *Rev. Mod. Phys.* **73** 515
[44] Perdew J P, Burke K and Ernzerhof M 1996 *Phys. Rev. Lett.* **77** 3865
[45] Corso A D 2014 *Comput. Mater. Sci.* **95** 337
[46] Eliashberg G M 1960 *Sov. Phys. JETP* **11** 696
[47] Allen P B 1972 *Phys. Rev. B* **6** 2577
[48] Lee K H, Chang K J and Cohen M L 1995 *Phys. Rev. B* **52** 1425
[49] Richardson C F and Ashcroft N W 1997 *Phys. Rev. Lett.* **78** 118
[50] Hayward M A and Rosseinsky M J 2003 *Solid State Sci.* **5** 839